

## Supplementary material

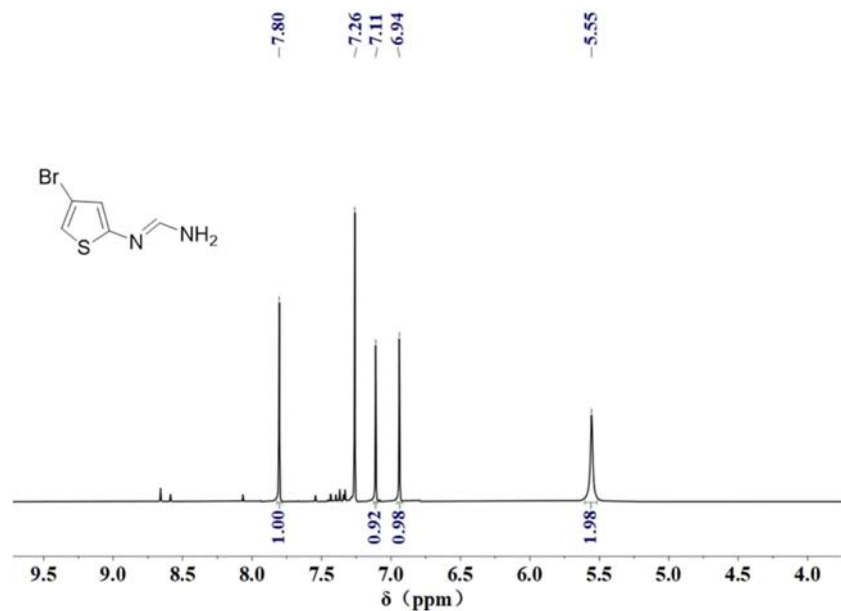


Figure S1:  $^1\text{H}$  NMR spectrum of A2.

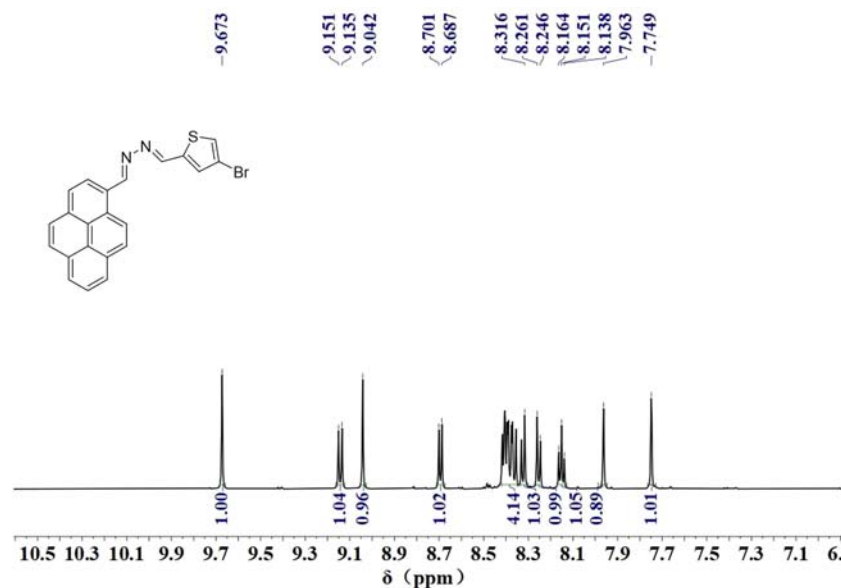
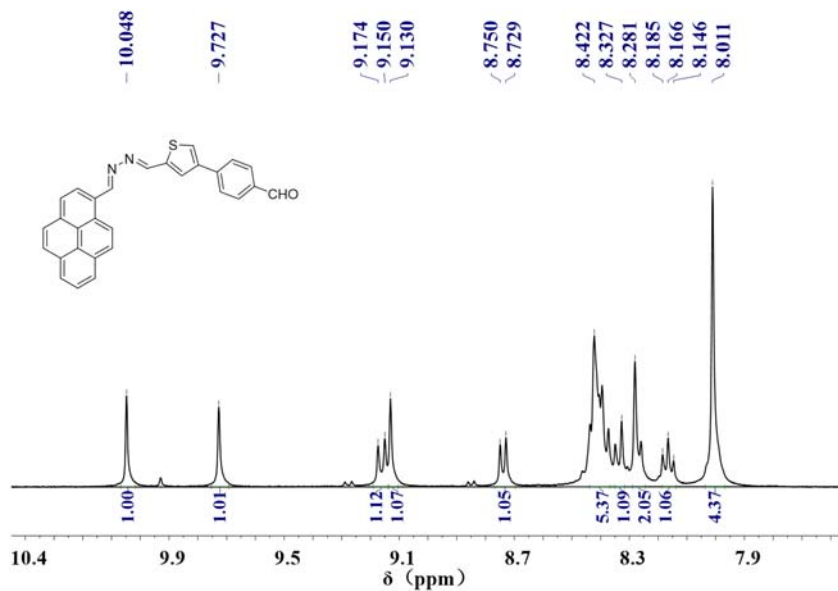
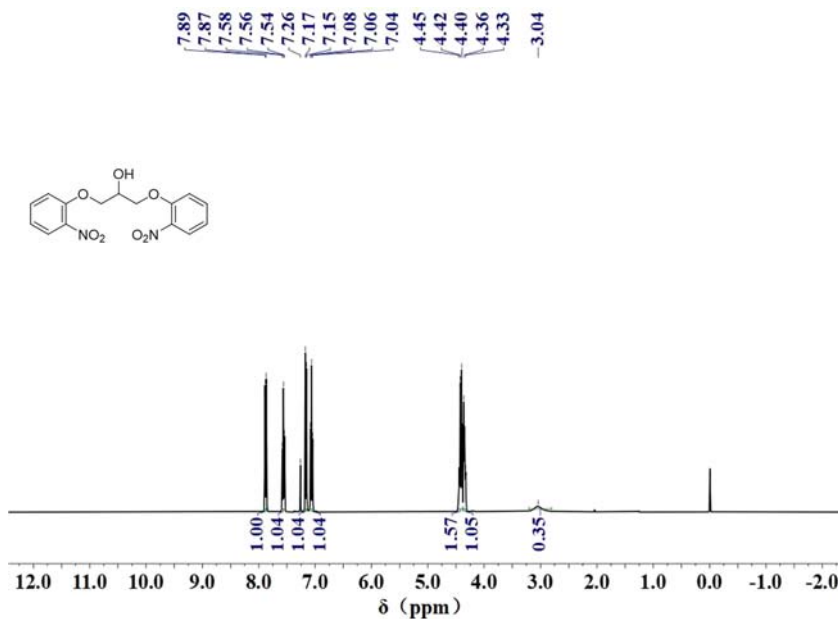


Figure S2:  $^1\text{H}$  NMR spectrum of A4.



**Figure S3:** <sup>1</sup>H NMR spectrum of A6.



**Figure S4:** <sup>1</sup>H NMR spectrum of B3.

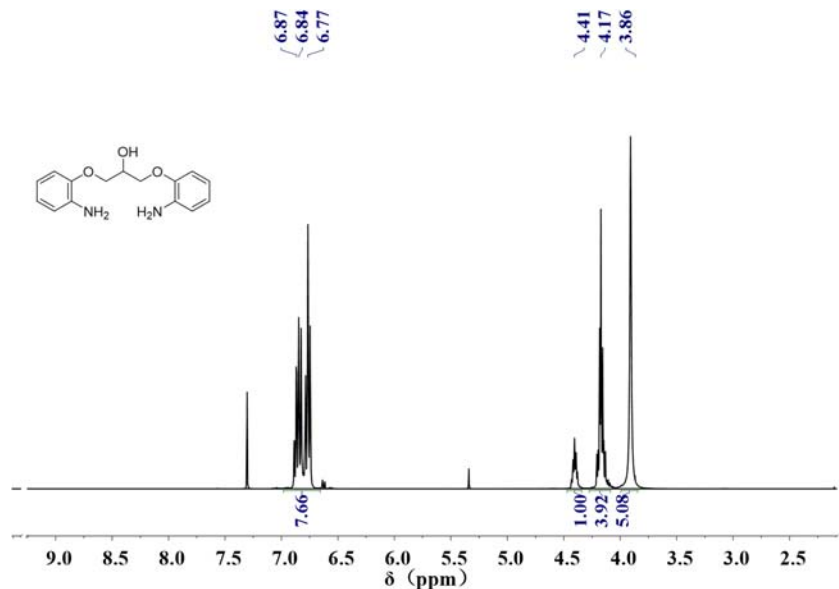


Figure S5: <sup>1</sup>H NMR spectrum of B4.

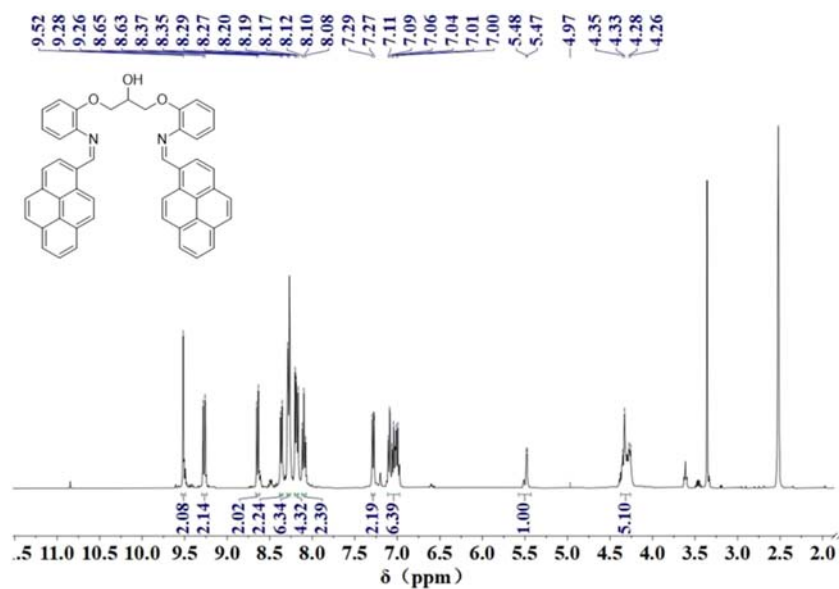


Figure S6: <sup>1</sup>H NMR spectrum of B5.

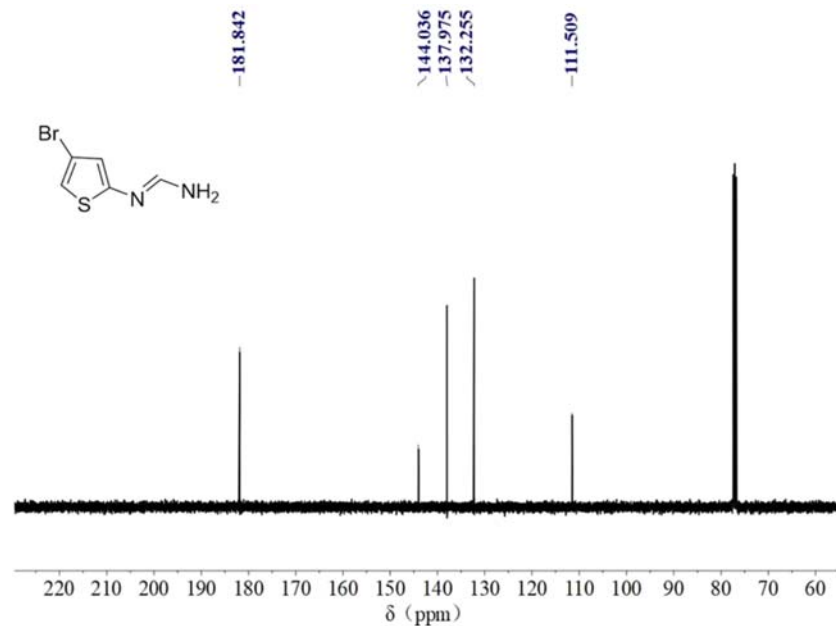


Figure S7:  $^{13}\text{C}$  NMR spectrum of A2.

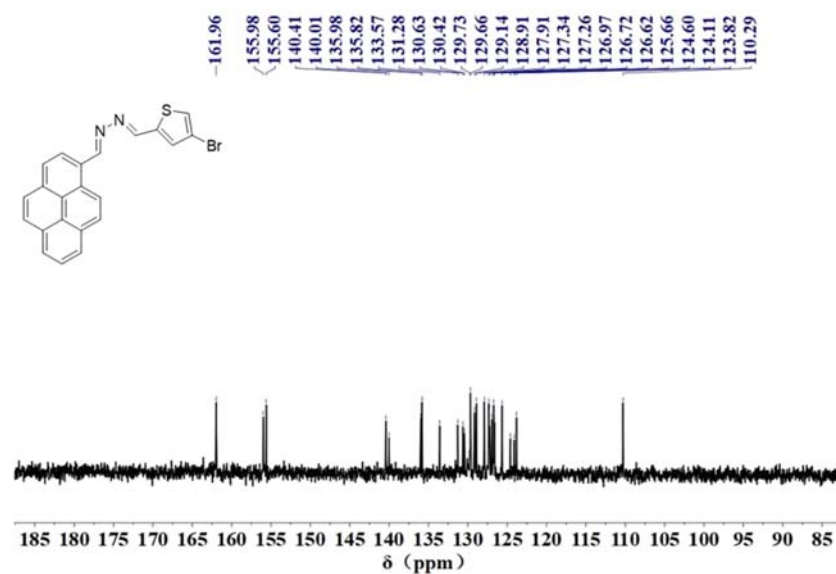


Figure S8:  $^{13}\text{C}$  NMR spectrum of A4.

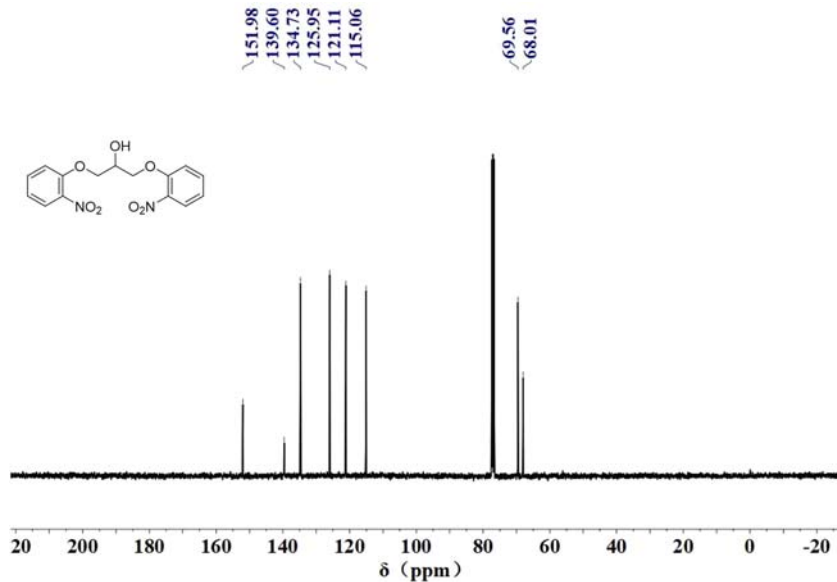


Figure S9:  $^{13}\text{C}$  NMR spectrum of B3.

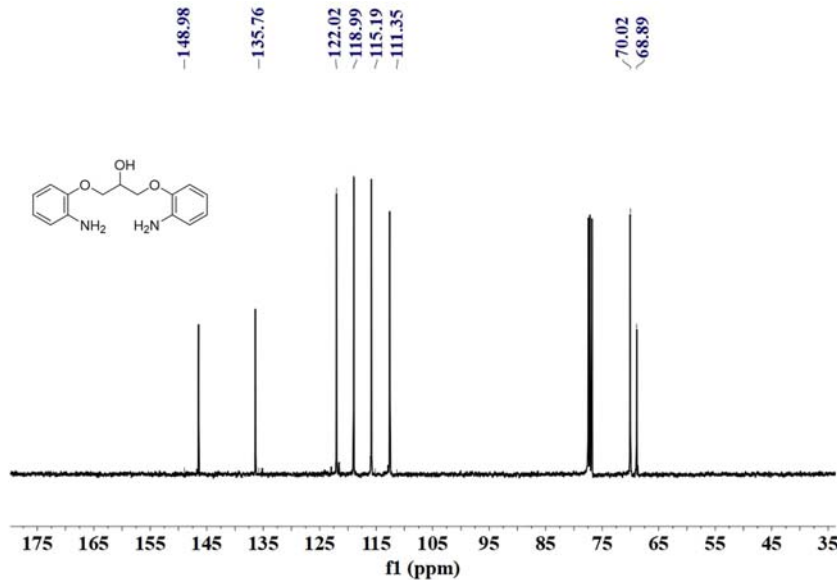


Figure S10:  $^{13}\text{C}$  NMR spectrum of B4.

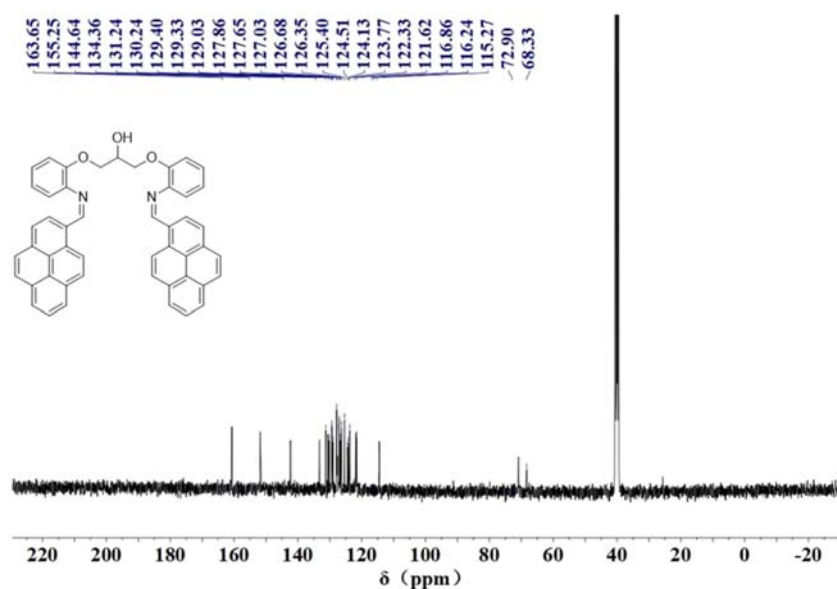


Figure S11:  $^{13}\text{C}$  NMR spectrum of B5.

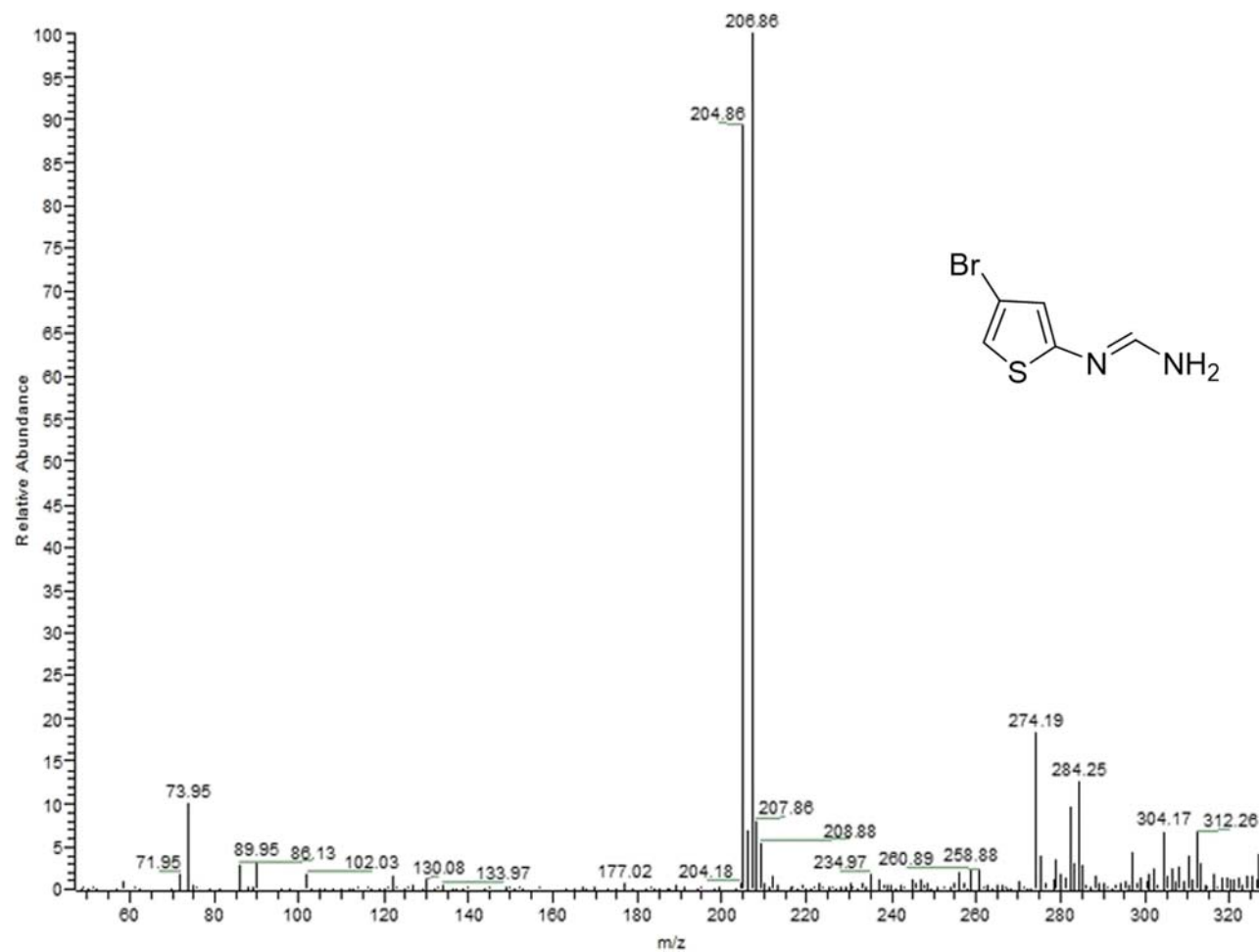


Figure S12: MS spectrum of A2.

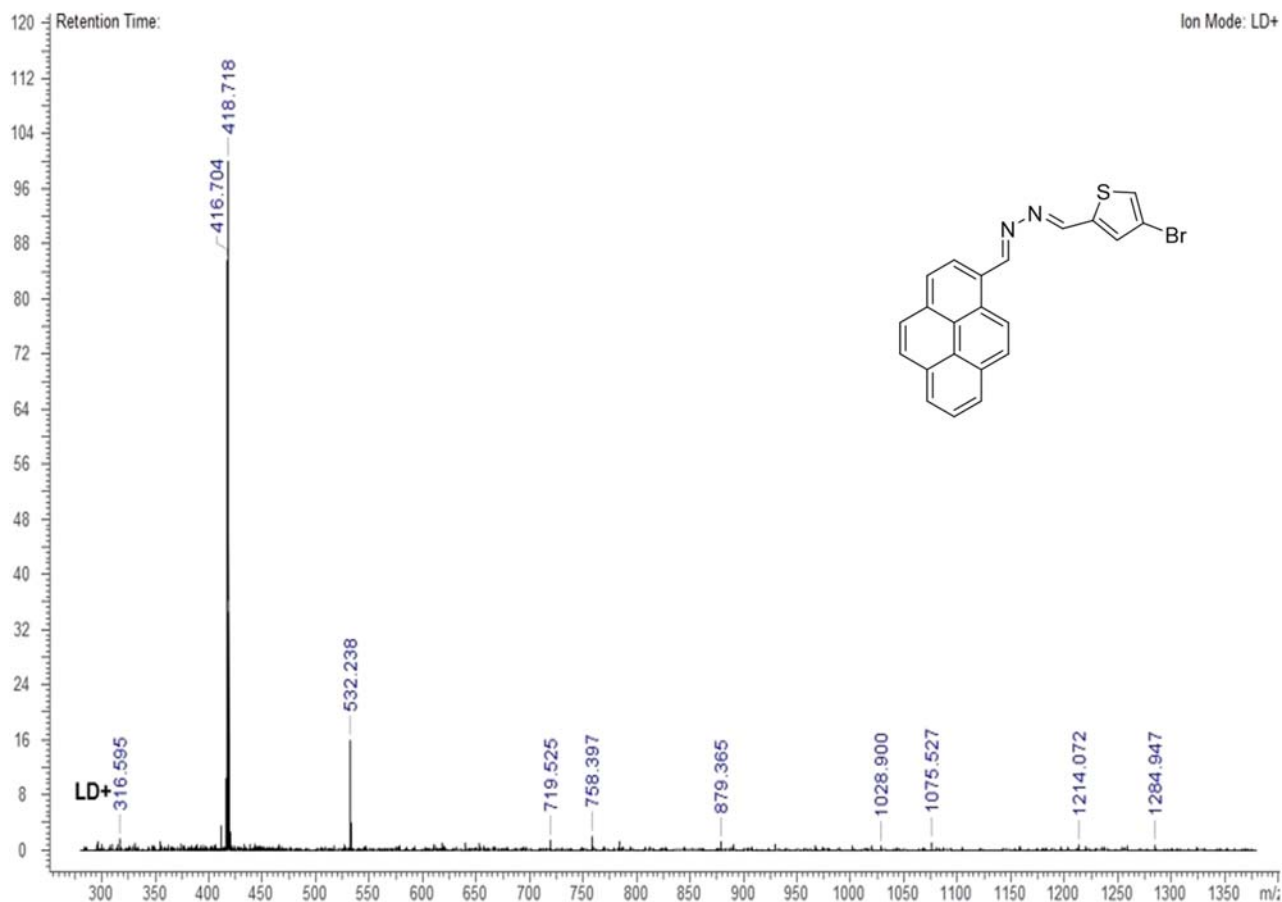


Figure S13: MS spectrum of A4.

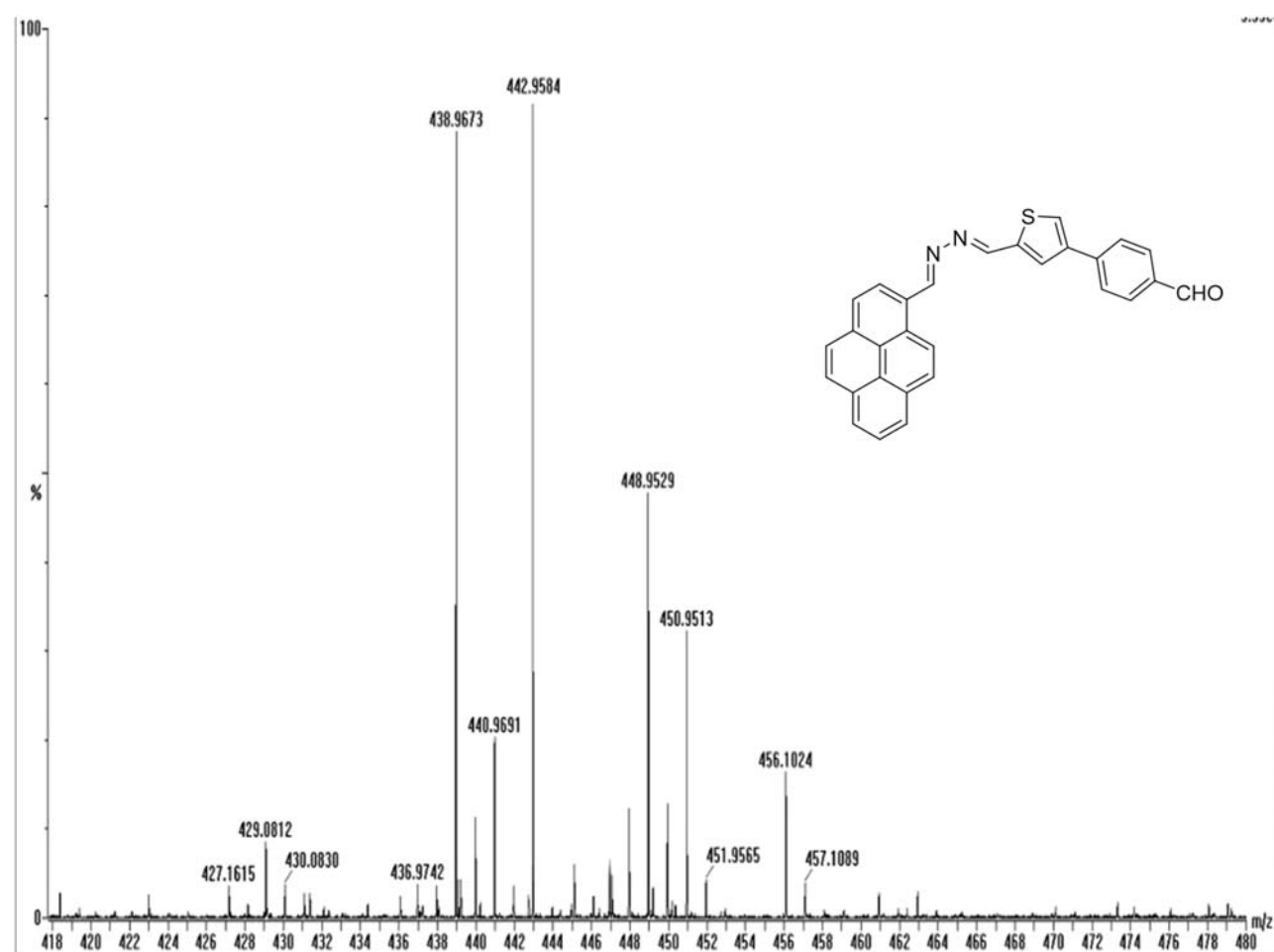


Figure S14: MS spectrum of A6.

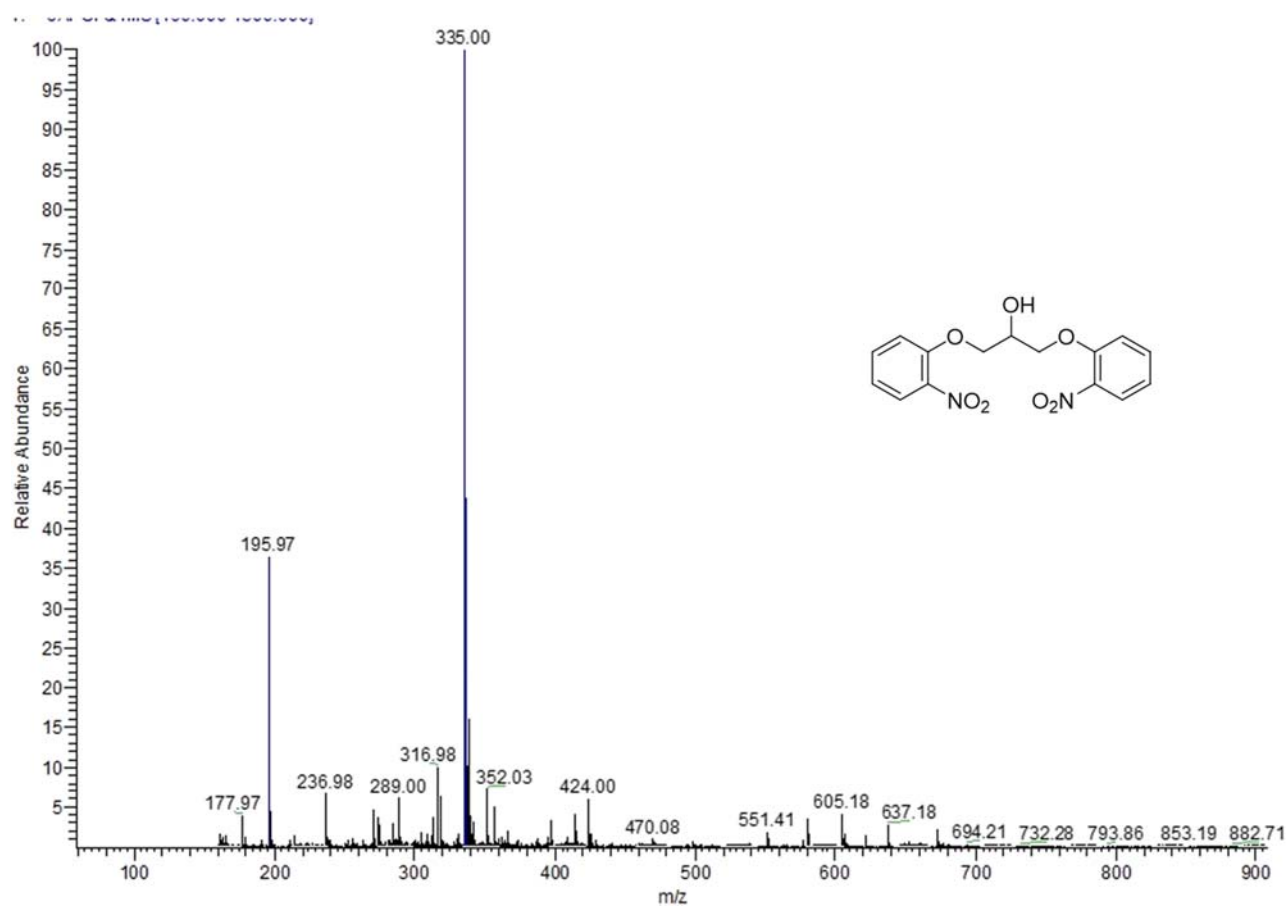


Figure S15: MS spectrum of B3.

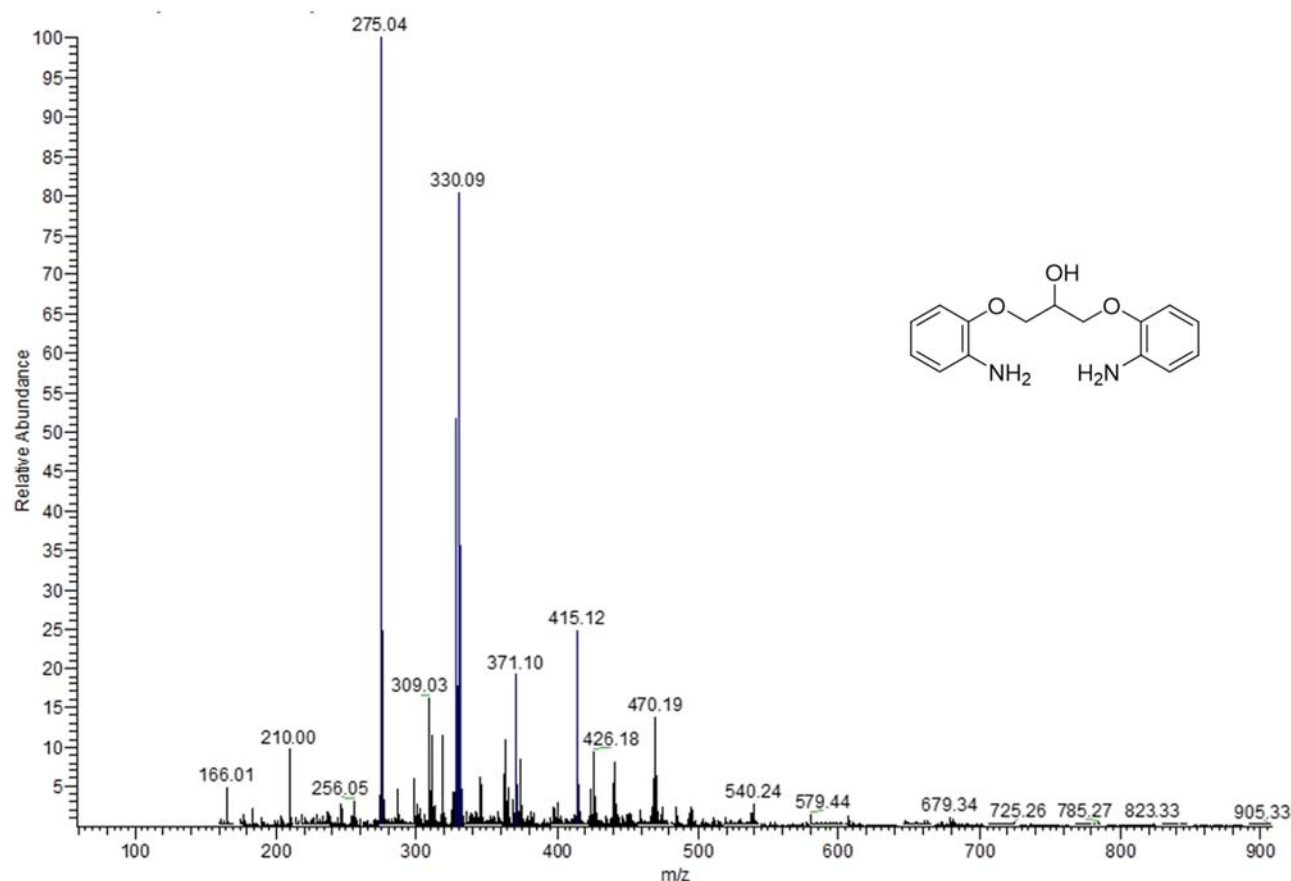
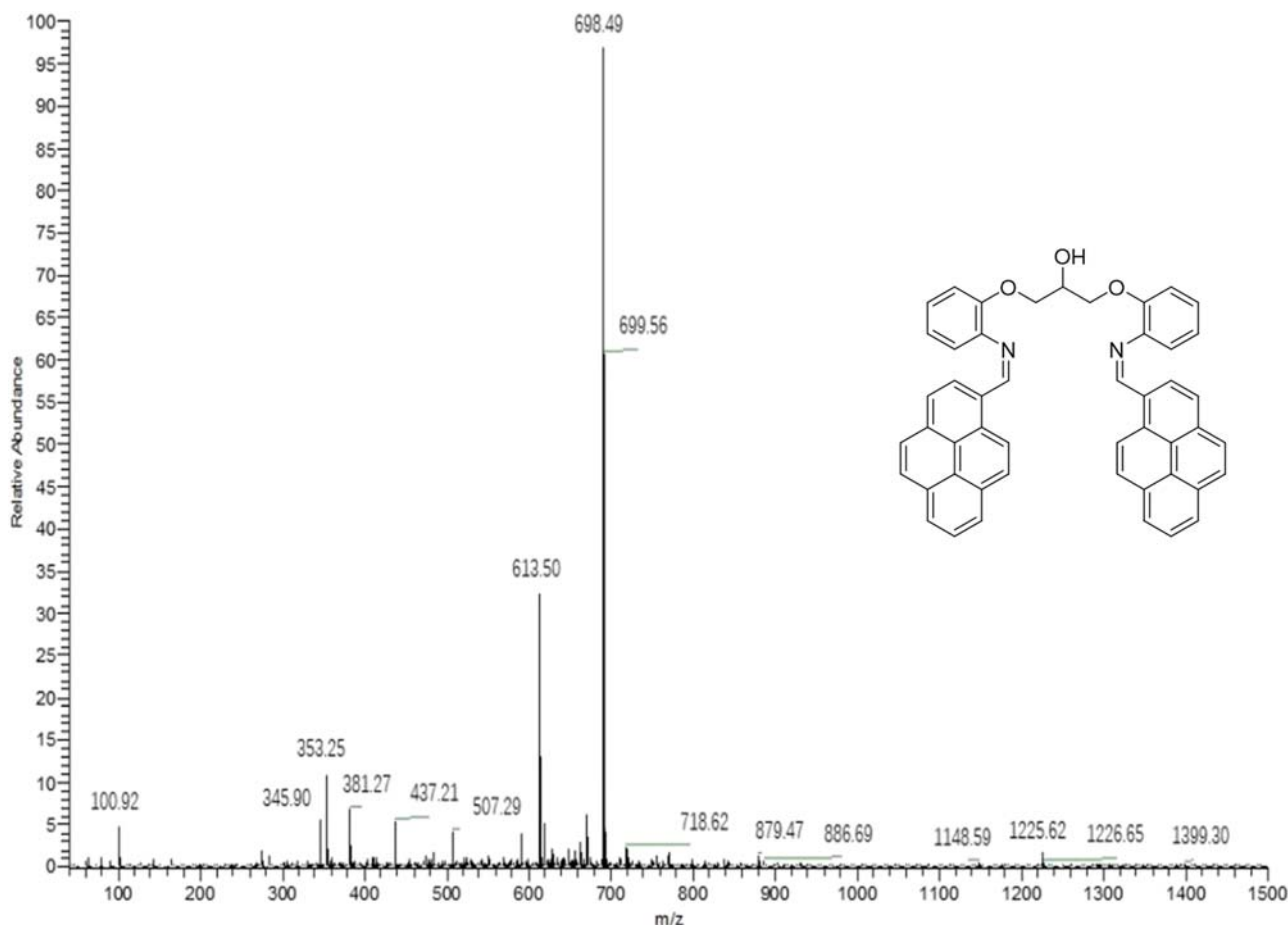
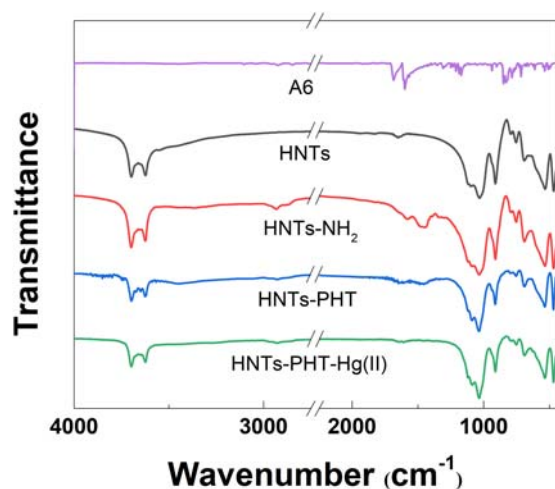


Figure S16: MS spectrum of B4.



**Figure S17:** MS spectrum of B5.



**Figure S18:** FTIR spectra of A6, HNTs, HNTs-NH<sub>2</sub>, HNTs-PHT and HNTs-PHT-Hg(II).

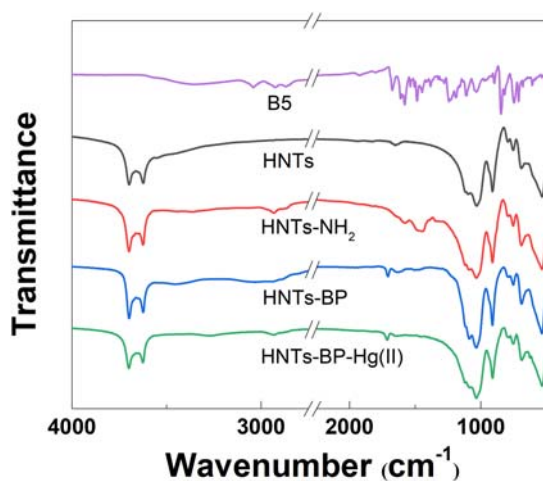


**Figure S19:** FTIR spectra of B5, HNTs, HNTs-NH<sub>2</sub>, HNTs-BP and HNTs-BP-Hg(II).

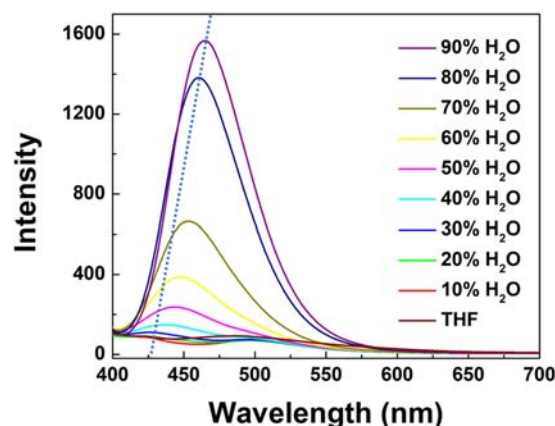


**Figure S20:** Fluorescence spectra of HNTs-PB as a function of increasing water content (0–90%).

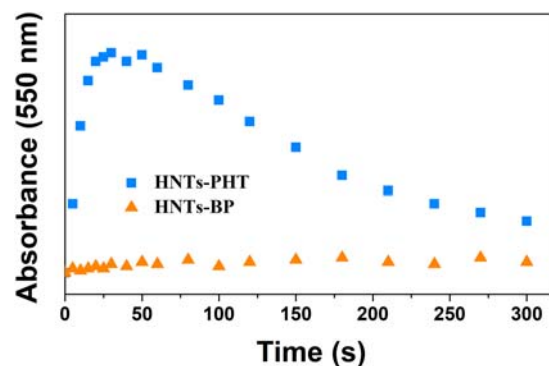


**Figure S22:** Absorbance at 550 nm vs time of the interaction between Hg(II) with HNTs-PHT or HNTs-BP.

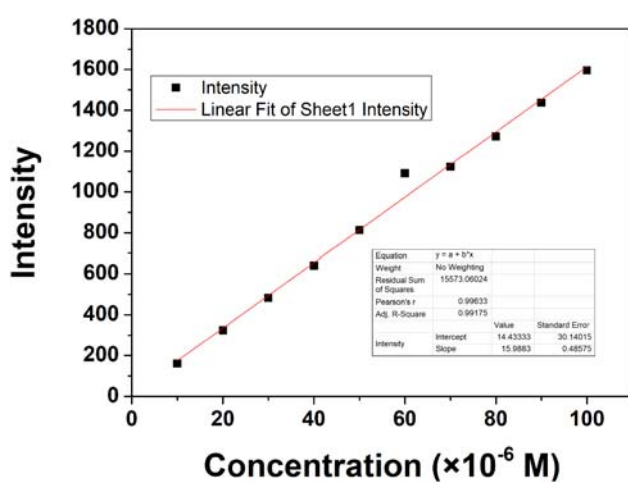


**Figure S21:** Linear regression for fluorescence intensity and concentration of Hg(II).

**Table S1:** Comparison on the detection and separation of Hg(II) methods in literature

Ref. no.	Detection method	Separation method	Interfering ions	Specificity over other ions	
[1]	UV lamp and color change	Adsorption by silicate derivatives	Cu <sup>2+</sup>	Na <sup>+</sup> , K <sup>+</sup> , Ca <sup>2+</sup> , Mg <sup>2+</sup> , Co <sup>2+</sup> , Ni <sup>2+</sup> , Cu <sup>2+</sup> , Zn <sup>2+</sup> , Al <sup>3+</sup> , Fe <sup>2+</sup> , Fe <sup>3+</sup> , Pb <sup>2+</sup> , Ag <sup>+</sup> , Cd <sup>2+</sup>	
[2]	Addition of active additive and UV analysis	Cloud point extraction	Not find	Not evaluated	
[3]	Resonance light scattering spectrometry	Adsorption by gold nanoparticles	Not find	Ba <sup>2+</sup> , Zn <sup>2+</sup> , Na <sup>+</sup> , and Fe <sup>3+</sup>	
[4]	Bio-inspired colorimetric detection	Adsorption by magnetic particles	Pb <sup>2+</sup>	Not evaluated	
[5]	Heterogeneous colorimetric and spectrophotometric chemosensor	Adsorption by FMS-1	Not find	Not evaluated	
[6]	Membrane material adsorption	Adsorption by mesoporous silica	Ag <sup>+</sup>	Not evaluated	
[7]	Atomic absorption spectroscopy	Gold-nanoparticle-based graphite furnace	Cu <sup>2+</sup>	Not evaluated	
[8]	Fluorescence chemosensor	Adsorption by Fe <sub>3</sub> O <sub>4</sub> @SiO <sub>2</sub> -Au@PSiO <sub>2</sub>	Not find	Ni <sup>2+</sup> , Cd <sup>2+</sup> , Ca <sup>2+</sup> , Ba <sup>2+</sup> , Pb <sup>2+</sup> , Cu <sup>2+</sup> , Zn <sup>2+</sup> , Co <sup>2+</sup> , Mg <sup>2+</sup> , Ag <sup>+</sup> , Na <sup>+</sup> , K <sup>+</sup> , Li <sup>+</sup> , Co <sup>2+</sup> , Zn <sup>2+</sup> , Cu <sup>2+</sup> , Cd <sup>2+</sup> , Ca <sup>2+</sup> , Mg <sup>2+</sup> , Pb <sup>2+</sup>	
[9]	FT-IR	Adsorption by Bioinspired supramolecular fibers	Not find	Not evaluated	
[10]	Fluorescence change (“turn on”)	Adsorption by Silica Microsphere poly(acrylic acid) hydrogel coatin	Cd <sup>2+</sup> , Pb <sup>2+</sup>	Not evaluated	
[11]	X-ray photoelectron spectroscopy	Not find	Cu <sup>2+</sup> , Cd <sup>2+</sup> and Pb <sup>2+</sup>	Not evaluated	
[12]	X-ray photoelectron spectroscopy	Adsorption by organic frameworks	Na <sup>+</sup> , Cd <sup>2+</sup> , Zn <sup>2+</sup> , Ni <sup>2+</sup> , Pb <sup>2+</sup> , Mg <sup>2+</sup> , Cr <sup>3+</sup>		
[13]	Fluorescence change (“turn on”)	Absorption by functionalized Fe <sub>3</sub> O <sub>4</sub> @SiO <sub>2</sub>	Not find	Cu <sup>2+</sup> , Ag <sup>+</sup> , Cd <sup>2+</sup> , Sr <sup>2+</sup> , Pb <sup>2+</sup> , Co <sup>2+</sup> , Fe <sup>2+</sup> , Fe <sup>3+</sup> , Mg <sup>2+</sup> , Na <sup>+</sup> , Ni <sup>2+</sup> , Zn <sup>2+</sup> , Ba <sup>2+</sup> , Al <sup>3+</sup>	
[14]	Color change	Absorption by mesoporous silica probes	Fe <sup>3+</sup>	Na <sup>+</sup> , Mg <sup>2+</sup> , Al <sup>3+</sup> , K <sup>+</sup> , Ca <sup>2+</sup> , Cr <sup>3+</sup> , Mn <sup>2+</sup> , Fe <sup>3+</sup> , Co <sup>2+</sup> , Ni <sup>2+</sup> , Cu <sup>2+</sup> , Zn <sup>2+</sup> , As <sup>3+</sup> , Cd <sup>2+</sup> , Pb <sup>2+</sup>	
[15]	Fluorescence change (“turn on”)	Precipitation separation	Not find	Fe <sup>3+</sup> , Co <sup>2+</sup> , Ni <sup>2+</sup> , Cu <sup>2+</sup> , Zn <sup>2+</sup> , Pb <sup>2+</sup> , Cd <sup>2+</sup>	

## Reference

- [1] Razi SS, Ali R, Srivastava P, Misra A. Smart excimer fluorescence probe for visual detection, cell imaging and extraction of  $\text{Hg}^{2+}$ . *RSC Adv.* 2015;5(97):79538–47.
- [2] Niazi A, Momeni-Isfahani T, Ahmari Z. Spectrophotometric determination of mercury in water samples after cloud point extraction using nonionic surfactant Triton X-114. *J Hazard Mater.* 2009;165(1–3):1200–3.
- [3] Fan Y, Yun FL, Yuan FL. A sensitive resonance light scattering spectrometry of trace  $\text{Hg}^{2+}$  with sulfur ion modified gold nanoparticles. *Anal Chim Acta.* 2009;653(2):207–11.
- [4] Knecht MR, Sethi M. Bio-inspired colorimetric detection of  $\text{Hg}^{2+}$  and  $\text{Pb}^{2+}$  heavy metal ions using Au nanoparticles. *Anal Bioanal Chem.* 2009;394:33–46.
- [5] Kim E, Cho N, Vittal JJ, Lee SS, Han WS, Jung JH. A novel heterogeneous colorimetric and spectrophotometric chemosensor for detection and adsorption of  $\text{Hg}^0$  and  $\text{Hg}^{2+}$ . *J Nanosci Nanotechnol.* 2010;10(8):4914–20.
- [6] Zou Q, Zou L, Tian H. Detection and adsorption of  $\text{Hg}^{2+}$  by new mesoporous silica and membrane material grafted with a chemodosimeter. *J Mater Chem.* 2011;21(38):14441–7.
- [7] Hsu IH, Hsu TC, Sun YC. Gold-nanoparticle-based graphite furnace atomic absorption spectrometry amplification and magnetic separation method for sensitive detection of mercuric ions. *Biosens Bioelectr.* 2011;26(11):4605–9.
- [8] Lv Q, Li G, Cheng Z, Lu H, Gao X. Magnetically recoverable fluorescence chemosensor for the adsorption and selective detection of  $\text{Hg}^{2+}$  in water. *Environ Sci Process Impacts.* 2013;16:116–23.
- [9] Wang YS, Cheng CC, Chen JK, Ko FH, Chang FC. Bioinspired supramolecular fibers for mercury ion adsorption. *J Mater Chem A Mater Energy Sustain.* 2013;1(26):7745–50.
- [10] Ding Y, Zhu W, Xu Y, Qian X. A small molecular fluorescent sensor functionalized silica microsphere for detection and removal of mercury, cadmium, and lead ions in aqueous solutions. *Sens Actuators B Chem.* 2015;220:762–71.
- [11] Xu L, Liu N, Cao Y, Lu F, Chen Y, Zhang X, et al. Mercury ion responsive wettability and oil/water separation. *ACS Appl Mater Interfaces.* 2014;6(16):13324–9.
- [12] Ge J, Xiao J, Liu L, Qiu L, Jiang X. Facile microwave-assisted production of  $\text{Fe}_3\text{O}_4$  decorated porous melamine-based covalent organic framework for highly selective removal of  $\text{Hg}^{2+}$ . *J Porous Mater.* 2016;23(3):791–800.
- [13] Tian Y, Shi W, Luo J, Ma F, Mi H, Lei Y. Carbazole-based conjugated polymer covalently coated  $\text{Fe}_3\text{O}_4$  nanoparticle as efficient and reversible  $\text{Hg}^{2+}$  optical probe. *J Polym Sci Part A Polym Chem.* 2013;51(17):3636–45.
- [14] Das T, Singha D, Pal A, Nandi M. Mesoporous silica based recyclable probe for colorimetric detection and separation of ppb level  $\text{Hg}^{2+}$  from aqueous medium. *Sci Rep.* 2019;9(1):19378–88.
- [15] Halder U, Lee HI. BODIPY-derived polymeric chemosensor appended with thiosemicarbazone units for the simultaneous detection and separation of  $\text{Hg}(\text{II})$  ions in pure aqueous media. *ACS Appl Mater Interfaces.* 2019;11(14):13685–93.